Transactions of NAMP 20, 1 (2024) 9-22

Transactions of
The Nigerian Association of
Mathematical Physics
Journal homepage: https://nampjournals.org.ng

Predictive Accuracy and Transferability of a Newly Proposed Traffic Flow Model and Selected Models

Mabur Yaks Mafuyai[a*]; Dirting Dakup Bakwa[a]; and Yakubu Yerima Jabil[a]

[a] *Department of Physics, Faculty of Natural Sciences, University of Jos.*

https://doi.org/10.60787/tnamp-v20-351

ARTICLE INFO

Article history:
Received xxxxx
Revised xxxxx
Accepted xxxxx
Available online xxxxx

Keywords:
Fundamental diagram,
Traffic flow,
Cross-validation,
Flow-Density model,
Mathematical model.

ABSTRACT

Over the past eight decades, functional forms of an empirical macroscopic fundamental diagram have been continually proposed yet the predictive power of most models at mid and high densities continuous to be questionable to the traffic flow research community. K-fold cross-validation was used to assess and compare the predictive performance of some macroscopic equilibrium fundamental diagram with a newly proposed model. The results reveal that the newly proposed model perform better than the other models in predicting traffic states, particularly, in mid and high densities. This shows that the proposed model could be useful for extrapolation of traffic states at mid and high densities. Furthermore, the proposed model shows consistently good performance across various roads despite its few parameters. This proves that the proposed model has high flexibility that enables it to adapt to most of the trends of traffic data. It is therefore concluded that a single-regime model with few parameters is capable of accurately describing empirical fundamental diagram.

1.0 Introduction

Mathematical models are developed to among other things help in predicting the future states of the physical system that they represent. Traffic flow models play significant role in this respect because traffic flow data is rarely complete across all density ranges, hence the need to interpolate or extrapolate traffic states. To achieve this, a traffic flow model needs to easily generalize, i.e. it should be able to predict test data with good accuracy. Therefore, traffic flow models are required not to under fit or over fit any given data set if they most easily generalize across data sets. applicable on roads with different flow characteristics. This property is known as model's transferability.

[*]Corresponding author.: Mabur Yaks Mafuyai
E-mail address: mafuyaim@unijos.edu.ng

Equally, a traffic flow model is expected to perform well on different road facilities, i.e. it should be This is important because traffic data from different roads can be different in both quality and quantity. The road geometry, existence of intersections, use of traffic control infrastructure, method of data collections and aggregation, etc. affect the nature of traffic data and hence it is not uncommon to see models that perform well on a given data set perform poorly on another.

Traffic flow model can be classified as equilibrium models or non-equilibrium models. The equilibrium models represent traffic state when the rates of change of speed and density are zero. One of the most studied classes of equilibrium traffic flow model is macroscopic fundamental diagram. Empirical macroscopic fundamental diagram is the graphic representation of the relationship between the variables (flow, speed, and density) that give the collective behavior of a traffic state observed in real-world. The functional form of an empirical macroscopic fundamental diagram is a mathematical model that seeks to represent the macroscopic fundamental diagram accurately. Over the past eight decades, functional form of an empirical macroscopic fundamental diagram have been continually proposed yet the predictive power of most models at mid and high densities continuous to be questionable to the traffic flow research community (see Fig.1 for the graphs of some single-regime models). It can be noticed from Fig.1 that most of the single-regime models tend to overestimate traffic states at mid densities (30-80veh/km) but under estimate traffic states at high densities (80veh/km and above). For this and many other reasons, the search for an accurate traffic flow model has persisted [1], [2], [3], [4]. Recently, a new traffic flow model has been proposed [5] and the aim of this research is investigate and compare the predictive power and transferability of the proposed model with some selected models. The rest of the paper is organized as follows, section 2 provide the literature review traffic flow models, section 3 outlines the methodologies employed in the study, section 4 presents the findings, and section 5 presents the result discussion and conclusions.

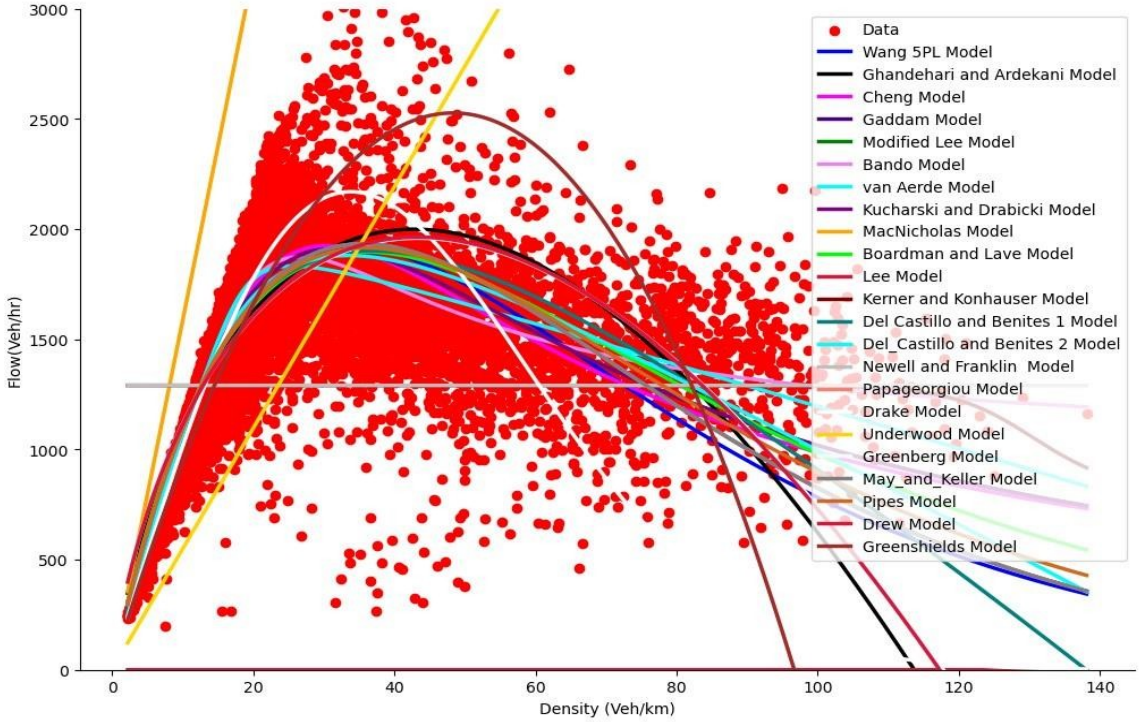

Fig.1. Graph of some Single-Regime Traffic Flow Models Showing Poor Performance at Mid and High Densities

2. Literature Review

The debate on the formulation of the functional form of an empirical fundamental diagram has been whether the empirical fundamental diagram should be described accurately by a single function or multiple functions representing different regions on the fundamental diagram. Two schools of thought exist, those that believe the fundamental diagram is continuous and hence can be represented by a single function [6], [7] and those

that believe that discontinuity exist and hence there is need for two or more functions [8], [9], [10] to correctly represent empirical fundamental diagram. Moreover, multi-regime models lack mathematical tractability and elegance; hence the search for a suitable functional form of a single-regime model has persisted.

2.1 Single-Regime Fundamental Diagram

Single-Regime fundamental diagrams are fundamental diagrams represented by a single mathematical expression. Their greatest attraction is mathematical elegance [11]. Table 1 presents some of the single-regime fundamental diagrams. Each of these fundamental diagrams is deficient in one way or the other [1], [2], [4], [12], [13] and their ability to represent the empirical data at mid and high densities is poor (Figure 1). Some of the most recently proposed single-regime models include Five-Parameter logistic model by Wang et al. [11], longitudinal control model by Ni et al. [14], Kucharski & Drabicki [15], Modified Lee, and Gaddam & Rao [4], and Cheng et al., [2].

Wang et al. [11] was motivated by the success of generalized logistic equation in other fields of research that modeled biological growth patterns. And by observing the trend of speed-density scattered plot of GA400 data set and comparing it to the trends often modeled by logistic equation, Wang et al. [11] proposed a five-parameter logistic speed-density model. Relative to the existing single-regime models, the five-parameter logistic model shows good performance across all density range. However, the model is deficient in predicting jam density, it does not have a simple analytic expression for critical density, and has some parameters that are difficult to determine as admitted by the authors. Furthermore, Bramich et al., [1] pointed out that the authors erroneously associate one of the model's parameters with free-flow speed. Hence, the only physical parameters in the model are two and not three as presented by the authors. Another downside of the five-parameter logistic model was observed by Cheng et al. [2]and Romanowska & Jamroz [13]; that the model's flow-density and speed-flow functions possess undesirable backward-bending phenomenon at high densities. In line with the argument for the need for mathematical elegance and accuracy and motivated by the limitations of the five-parameter logistic models, Gaddam & Rao [4] proposed two models – Modified Lee model and a new model. While some of the limitations of the five-parameter logistic model are overcomed by the Gaddam & Rao [4] proposed models, the empirical accuracy of the models was not better than that of the five-parameter logistic model. In 2016, Ni et al. [14] presented a longitudinal control model (LCM) with four physically meaningful parameters – free-flow speed, aggressiveness, average response time, and effective vehicle length. The model shows good performance on real world data and outperformed other models compared with it. Another interesting part of LCM is its ability to produce various shapes of the fundamental diagram of interest in the literature which include reverse-lambda, triangular and skewed parabola. However, the LCM has no simple analytic expression for capacity which is acknowledged by the authors. Equally, the authors appreciated the fact that LCM could not realize reasonable capacity and accuracy at both free flow and congested flow regimes concurrently in some instances. Similarly, a closer look at Figure 3 to 8 in the work of Ni et al. [14] would reveal instances of over-estimation or under-estimation at some density ranges which could affect the model's predictive power (Wang et al., 2022). In an attempt to improve the estimation method of macroscopic volume delay function (VDF), Kucharski & Drabicki [15] proposed a model which was studied in the context of fundamental diagram by Romanowska & Jamroz [13]. While the model showed reasonable performance relative to many other models except Wang's five-parameter logics model, it still falls short of standard in a number of ways. For instance, the model does not predict jam density and it is not bounded below. Recently, Cheng et al. [2] proposed an S-shaped three-parameter model with aim of achieving mathematical elegance, accuracy and parsimony. The model was compared against some existing single-regime modes and the model shows good performance on empirical data and outperformed all other models except the five-parameter logistic model. The performance across all density ranges was good except at high densities, the flow-density model shows poor performance which the authors blamed on the use of only speed information in the objective function and suggested the use of both speed and flow information in the objective function. This suggestion results

in the compromise of the accuracy of the speed-density model. Furthermore, the model does not predict jam density and hence, the predicted speed interval has no lower bound.

Table 1

Some existing single-regime models available in the literature

Author(s)	Functional Form	Parameters
Greenshields, (1935)	$q = V_f\, k(1 - \frac{k}{k_j})$	V_f , k_j
Drew, (1968)	$q = V_f\, k[1 - (\frac{k}{k_j})^{m}]$	V_f , k_j , m
Pipes, (1967)	$q = V_f\, k\,(1 - \frac{k}{k_j})^{n}$	V_f , k_j , n
May & Keller, (1967)	$q = V_f\, k\,(1 - (\frac{k}{k_j})^{m})^{n}$	V_f , k_j , n, m
Jayakrishnan et al., (1995)	$q = k[(V_j + (V_f - V_j))\,(1 - \frac{k}{k_j})^{m}]$	V_f ,V_j , k_j , m
Greenberg, (1959)	$q = V_m\, k \ln \frac{k_j}{k}$	V_m , k_j
(Underwood, (1961)	$q = V_f\, k \exp^{-\frac{k}{k_m}}$	V_f , k_m
Drake et al., (1967)	$q = V_f\, k \exp^{[-\frac{1}{2}(\frac{k}{k_m})^{2}]}$	V_f , k_m
Papageorgiou et al., (1989)	$q = V_f\, k \exp^{[-\frac{1}{a}(\frac{k}{k_m})^{a}]}$	V_f , k_m , a
Franklin, (1961) and Newell, (1961)	$q = V_f\, k\,\{1 - \exp^{[-\frac{\lambda}{V_f}(\frac{1}{k} - \frac{k}{k_j})]}\}$	V_f , k_j , λ
Del Castillo & Benítez, (1995)	Exponential curve $q = V_f\, k\,\{1 - \exp^{[\frac{\lvert C_j \rvert}{V_f}(1 - \frac{k_j}{k})]}\}$ maximum sensitivity curve $q = V_f\, k\,\{1 - \exp^{1-\exp^{[\frac{\lvert C_j \rvert}{V_f}(\frac{k_j}{k} - 1)]}}\}$	V_f , k_j , C_j

(Kerner, & Konhauser, (1994)	$q = V_f\ [\frac{1}{1 + exp^{((\frac{k}{k_c} - c_1)/c_2)}} - c_3]$	$V_f, k_c, c_1, c_2, , c_3$ Fixed parameters in the their work were $c_1, c_2\ and\ c_3$
Lee et al., (1998)	$q = \frac{V_f k\ (1 - \frac{k}{k_j})}{1 + E\ (\frac{k}{k_j})^{\theta}}$	V_f, k_j, E, θ
Boardman & Lave, (1977)	$q = V_f k exp(-c_1 k) exp(-c_2 k^2)$	V_f, c_1, c_2
van Aerde, (1995)	$q = \frac{v}{c_1 + \frac{c_2}{V_f - v} + c_3 v}$ *or*	$V_f, c_1, c_2, , c_3$
	$q = \alpha\ (1 - \beta k - ((\gamma k - 1)^2 + \delta k^2)^{1/2})$ *Brahmic et al*, (2022)	$\alpha, \beta, \gamma, \delta$
Bando et al., (1995)	$q = V_f k\ (\frac{\tanh(c_1 k^{-1} - c_2) + \tanh c_2}{1 + \tanh c_2})$	V_f, c_1, c_2
Ghandehari, & Ardekani, (2008)	$q = c_1 k ln\ (\frac{k_j + c_2}{k + c_2})$	k_j, c_1, c_2
MacNicholas, (2008)	$q = V_f k \frac{1 - (\frac{k}{k_j})^n}{1 + c\ (\frac{k}{k_j})^n}, n \geq 1, c \geq 0$	V_f, k_j, c, n
Wang et al., (2011)	$q = k\ (V_b + \frac{V_f - V_b}{[1 + exp\ (\frac{k - k_t}{\theta_1})]^{\theta_2}})$	$V_f, V_b, k_t, \theta_1, \theta_2$
Modified Lee [4]	$q = V_f k \frac{(1 - (\frac{k}{k_j})^a)^b}{1 + E\ (\frac{k}{k_j})^{\theta}}$	$V_f, E, k_j, \theta, a, b$ Parameter b was fixed at 1
Gaddam & Rao, (2019)	$q = V_f k \frac{(e^{-(\frac{k}{k_c})^{(1+a)}} - e^{-(\frac{k_j}{k_c})^{(1+a)}})^b}{1 - e^{-(\frac{k_j}{k_c})^{(1+a)}}}$	V_f, k_c, k_j, a, b Parameter b was fixed at 1.
Ni et al., (2016)	$q = \frac{[\ v\ ]}{(\gamma v^2 + \tau v + l)\ [1 - \ln\ (1 - \frac{v}{V_f})]}$	V_f, γ, τ, l

Kucharski & Drabicki, (2017)	$q = \frac{V_f k}{1 + a\left(\frac{k}{k_c}\right)^b}$	V_f, k_c, a, b
Cheng et al., (2021)	$q = \frac{V_f k}{\left[1 + \left(\frac{k}{k_c}\right)^m\right]^{2/m}}$	V_f, k_c, m
Gazis et al., (1959)	$f_m\left(\frac{q}{k}\right) = c_1 f_l\left(\frac{1}{k}\right) + c_2$ $f_p(x) = \begin{cases} x^{1-p} & for\ p \neq 1 \\ \ln x & for\ p = 1 \end{cases}$	c_1, c_2, m, l m, *and* l are constants that define the form of sensitivity term

2.2 Multi-Regime Fundamental Diagram

Two considerations gave rise to multi-regime models: 1) the inability of the single regime models to accurately describe the fundamental diagram at all density ranges [35] and 2) the perceive discontinuity in the empirical fundamental diagram and the breakdown phenomenon experience in real situations [10]. Edie [9] was the first to propose a multi-regime fundamental diagram. Two mathematic functions were used in his work – Greenberg logarithmic function [22], used to describe congested regime and Underwood exponential function [23] used to describe free-flow regime. Since the work of Edie [9], many more multi-regimes have been proposed for various purposes. Some of these models are presented in Table 3. Apart from the fact that the multi-regime models do not always show superiority in fit accuracy statistically [36], their major drawback is lack of scientific means for selecting the regime boundaries [9], [37]. Another problem of multi-regime models is increased model complexity which might negatively affect its parsimony.

Table 2

Some multi-regime models available in the literature

Author(s)	Functional Form	Parameters
Edie, 1961[9]	$q = \begin{cases} V_f k \exp^{-\frac{k}{k_m}} & k < k_b \\ V_m k \ln \frac{k_j}{k} & k \geq k_b \end{cases}$	V_f, k_m, V_m, k_j, k_b
Drake et al., 1967[8]	$q = \begin{cases} V_f k - c k^2 & k \leq k_b \\ v_{bw} k - \left(\frac{v_{bw}}{k_j}\right) k^2 & k > k_b \end{cases}$	V_f, c, v_{bw}, k_j, k_b
Dick, 1966[38]	$q = \begin{cases} v_{bw} k(\ln k_j - \ln k_b) & k \leq k_b \\ v_{bw} k(\ln k_j - \ln k) & k > k_b \end{cases}$	v_{bw}, k_j, k_b
Munjal et al., 1971[39]	$q = \begin{cases} V_f k & k \leq k_m \\ v_{bw}(k_m - k) + V_f k_m & k > k_m \end{cases}$	V_f, v_{bw}, k_m
Smulder, 1989[40]	$q = \begin{cases} V_f k - \alpha k^2 & k \leq k_1 \\ \left(\frac{V_f k - \alpha k k_m}{\frac{1}{k_m} - \frac{1}{k_j}}\right)\left(\frac{1}{k} - \frac{1}{k_j}\right) & k > k_1 \end{cases}$	$V_f, k_m, \alpha, k_j, k_1$

May, 1990[41]	$q = \begin{cases} \alpha k - \beta k^2 & k \le k_b \\ \gamma k - \delta k^2 & k \ge k_b \end{cases}$	$\alpha, \beta, \gamma, \delta, k_b$
May, 1990[41]	$q = \begin{cases} \alpha k & k \le k_b \\ V_m k \ln \frac{k_j}{k} & k \ge k_b \end{cases}$	α, V_m, k_j, k_b
May, 1990[41]	$q = \begin{cases} \alpha k - \beta k^2 & k \le k_{b1} \\ \gamma k - \delta k^2 & k_{b1} \le k \le k_{b2} \\ \varepsilon k - \epsilon k^2 & k \ge k_{b2} \end{cases}$	$\alpha, \beta, \gamma, \delta, \varepsilon, \epsilon, k_{b1}, k_{b2}$
Daganzo, 1997[42]	$q = \begin{cases} V_f k & k < k_1 \\ V_f k_1 & k_1 < k < k_2 \\ q_m - \frac{k - k_1}{k_j - k_1} q_m & k \ge k_2 \end{cases}$	V_f, q_m, k_j, k_1, k_2
Triangular; Romanowska & Jamroz, 2021[13]	$q = \begin{cases} V_f k & k \le k_1 \\ q_m - \frac{k - k_m}{k_j - k_m} q_m & k \ge k_1 \end{cases}$	V_f, q_m, k_j, k_1, k_m
Wu, 2002[43]	$q = \begin{cases} k\left(v_0 - (v_0 - v_{k0})\left(\frac{k}{k_{k0}}\right)^{N-1}\right) & k \le k_{k0} \\ P_u k\left(v_0 - (v_0 - v_{k0})\left(\frac{k}{k_{k0}}\right)^{N-1}\right) + \frac{k}{\tau_{go}}\left(\frac{1}{k} - \frac{1}{k_j}\right)(1 - P_u) & k_{go,min} \le k \le k_{k0} \\ \frac{k}{\tau_{go}}\left(\frac{1}{k} - \frac{1}{k_j}\right) & k \ge k_{go,min} \end{cases}$ $where\ P_u = 1 - \left(\frac{k_{k0} - k_{go,min}}{k - k_{go,min}}\right)$ $k_{go,min} = \left[v_{k0}\left(\tau_{go} + \frac{1}{k_j v_{k0}}\right)\right]^{-1}$ $k_{ko} = \left[v_{k0}\left(\tau_{ko} + \frac{1}{k_j v_{k0}}\right)\right]^{-1}$	$v_0, v_{k0}, k_{k0}, k_j, \tau_{go}, \tau_{ko}$

3. Methodology

3.1 Models selection

The selected models include Edie multi-regime model, Drake's two-regime model, Wang et al five-parameter logistic model, van Aerde model, Gaddam model, Modified Lee's Model, Cheng et al model, and the newly proposed model [5]. The first four were considered because of their performance ranking according to the comprehensive comparative study by Bramich et al. [1], [12]while the last four are considered because they are relatively new and were not covered in the comparative study by Bramich et al. [1], [12].

3.2 Data preparation

To investigate predictive performance of each model, cross validation was used. The data was divided into two sets in the ratio of 70% to 30%. The 70% set was used to calibrate (train) the models and the 30% set

was used to test the models' predictions by calculating the root mean square error (RMSE) and plotting the scattered plot of the measured observation and the predicted together. To achieve a k-fold cross validation, four (k=4), different samples of 70% to 30% and 50% t0o 50% ratios were generated in the following manner:

1. 70-30, this was realized by taking the first 70% of the GA400 data as calibration set and last 30% as test set.
2. 30-70, this was realized by taking the first 30% of the GA400 data as test set and last 70% as calibration set
3. 15-70-15, this was realized by taking the first 15% and last 15% of the GA400 data and add it up to get 30% set for testing and the middle 70% constituted the calibration set
4. 50-50, this was realized by taking the first 50% of the GA400 data calibration set and last 50% as test set.

The RMSE for each pair was determined and the average value for the four different permutations was calculated and tabulated.

3.3 Models' transferability

To compare the transferability of the proposed model with some selected models by fitting the models to data from different roads. To achieve this objective, data from different region of the world were selected from Harvard Dataverse V1, available at https://dataverse.harvard.edu, Doi: 10.7910/DVN/FSGDGM provided by [44]. The following facilities were selected, Canada/Toronto/ N30431H2, France/Merseille/ 00034PMA0001, Germany/Hamburg/ K1225D3_2, Switzerland/Luzern/ ig11FD107_D3, France/Bodeaux/ Z28CT7, and France/Bodeaux/ Z224CT13. The models were fitted using Levenberg-Marquardt algorithm and the plots were generated using Matplotlib in python. The statistical metrics were determined using eqn. (1) and the error metrics were plotted for visualization.

$$\textit{Root mean sqaure error} \quad (RMSE) = \sqrt{\frac{1}{N}\sum_{i=1}^{N} (y_{ei}(k) - y_{mi}(k))^2} \quad (1)$$

4. Results

4.1 Predictive performance results

The root-mean square error (RMSE) of the testing set of each of the four samples were determined and tabulated in Table 3. And the plots are presented in Figure 2a to c.

Table 3

Root mean square errors for cross validation using LM and GA400 data

Train/Test Ratio	Proposed	Wang 5PL	Cheng	Gaddam	Modified Lee	van Aerde	Edie	Drake
70-30	121.99	132.57	127.69	142.47	128.47	1531.68	146.93	159.75
30-70	100.93	106.08	104.80	125.98	109.67	525.10	130.08	136.93
25-50-25	127.38	148.24	139.39	159.88	141.89	1335.75	165.84	171.32
50-50	125.28	137.16	131.94	148.11	133.53	1347.21	214.14	305.82
Average RMSE	**118.90**	**131.01**	**125.90**	**144.11**	**128.39**	**1184.93**	**164.2**	**193.46**

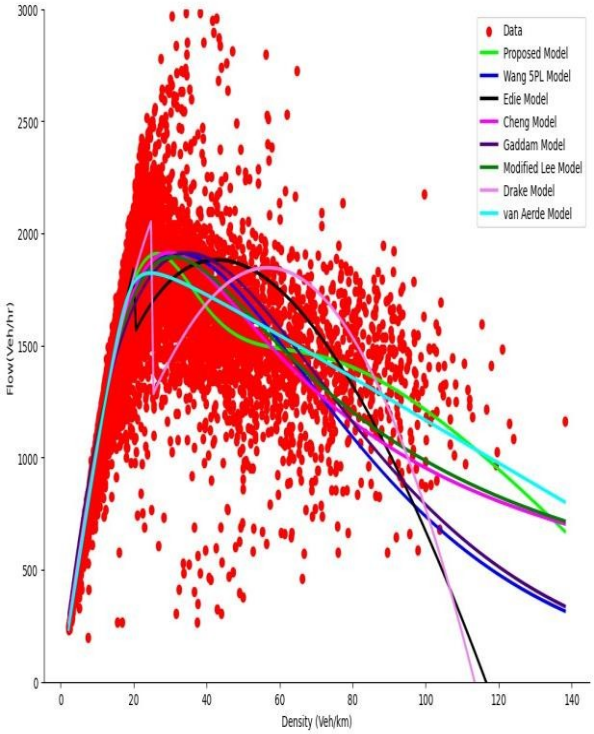

(a) Flow-density curves with 70% training data set

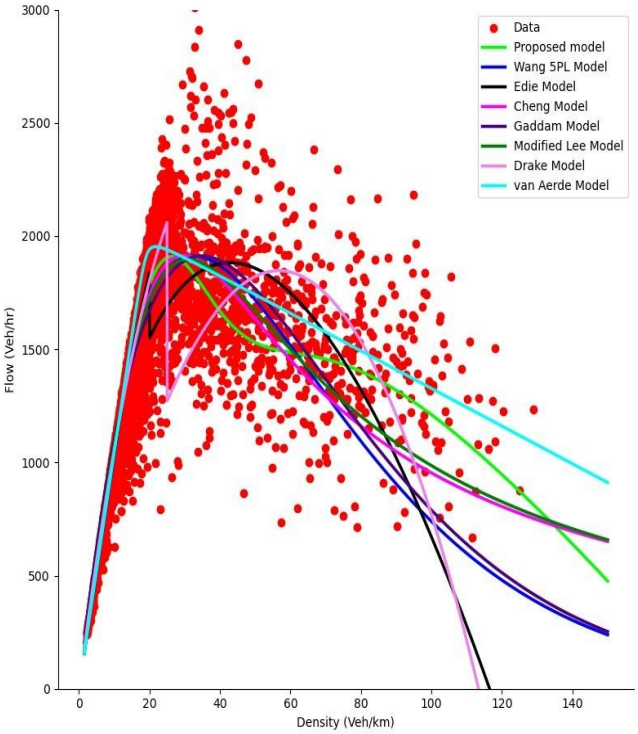

(b) Flow-density curves showing prediction of the 30% test data set

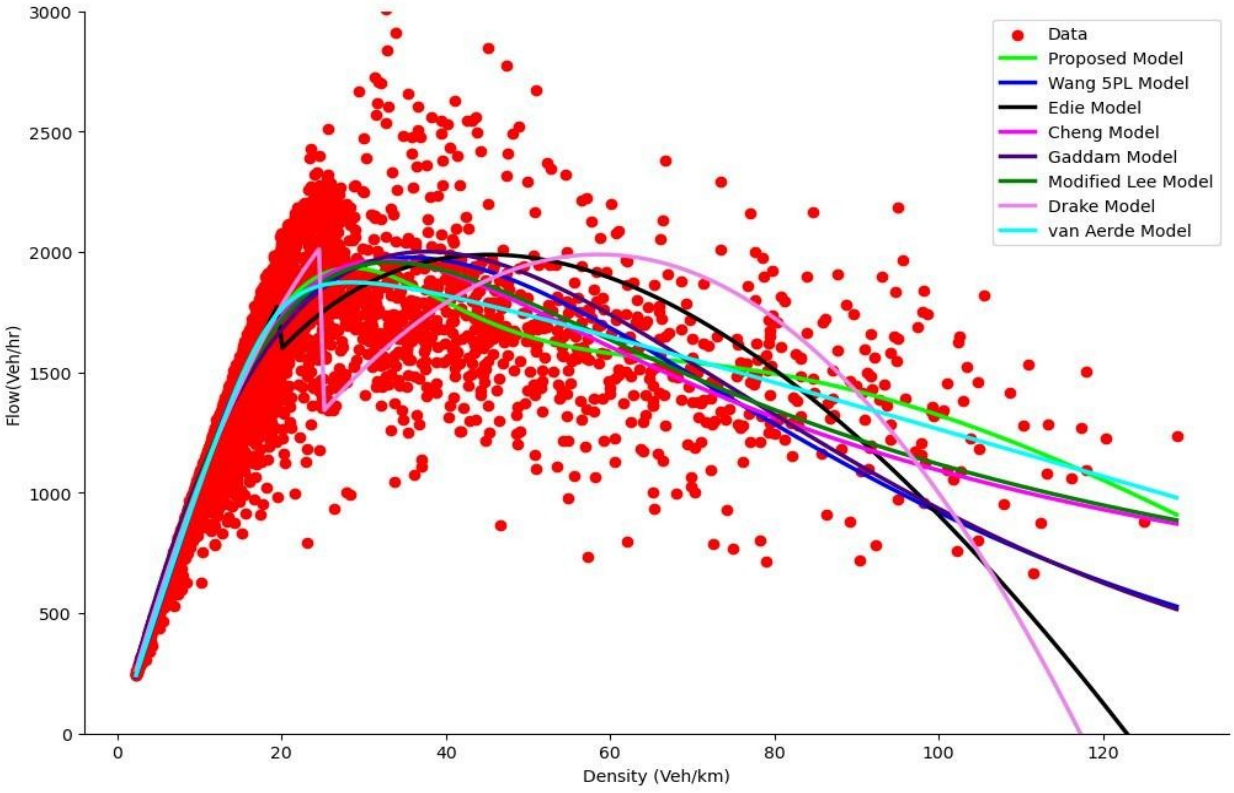

(c) The actual performances of the models on the 30% test data set

Fig. 2. Comparison of the predictive performance on test data

4.2 Results of Models' Transferability

The fitness accuracies are presented in Figure 3 while the graphs are presented in Figure 4a to g.

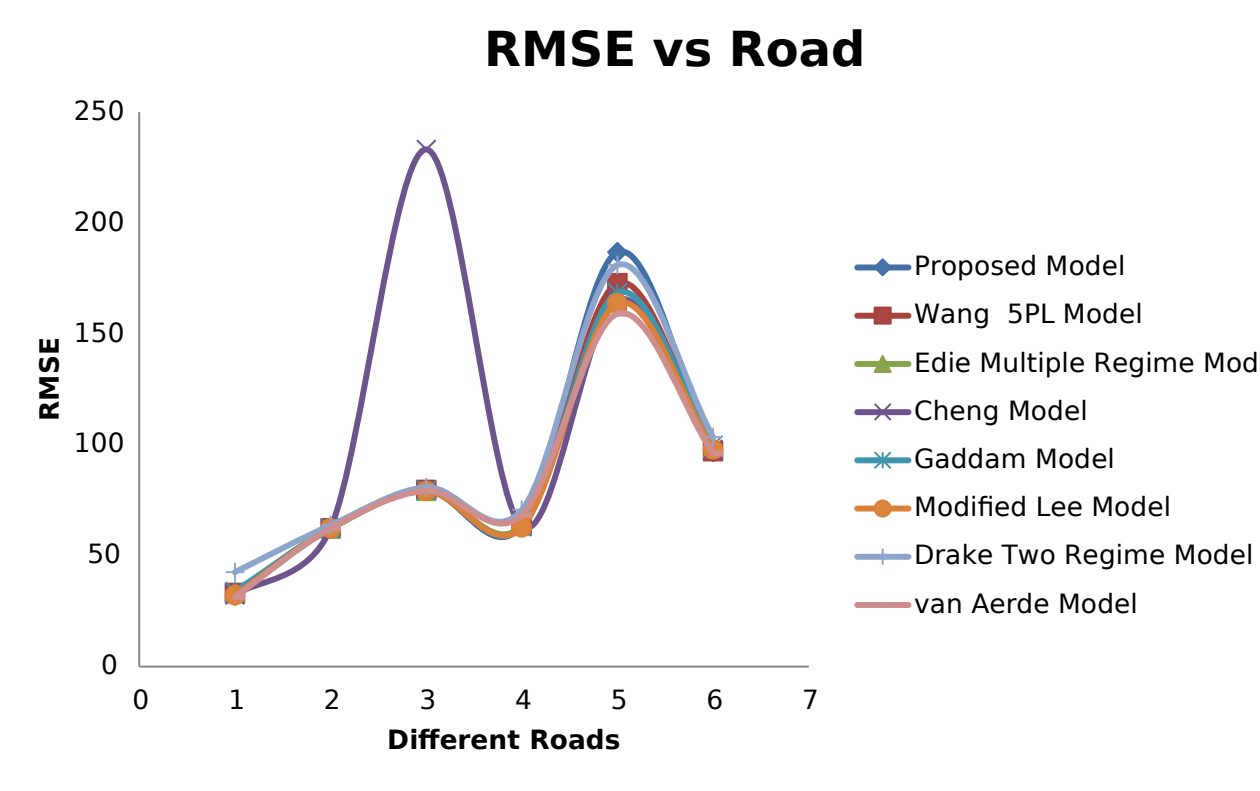

Note: 1=Canada/Toronto/N30431H2, 2=France/Merseille/00034PMA0001, 3=Germany/Hamburg/K1225D3_2, 4=Switzerland/Luzern/ ig11FD107_D3, 5=France/Bodeaux/ Z28CT7, 6=France/Bodeaux/ Z224CT13

Fig. 3. Graph of root mean square error of the models against roads from different cities

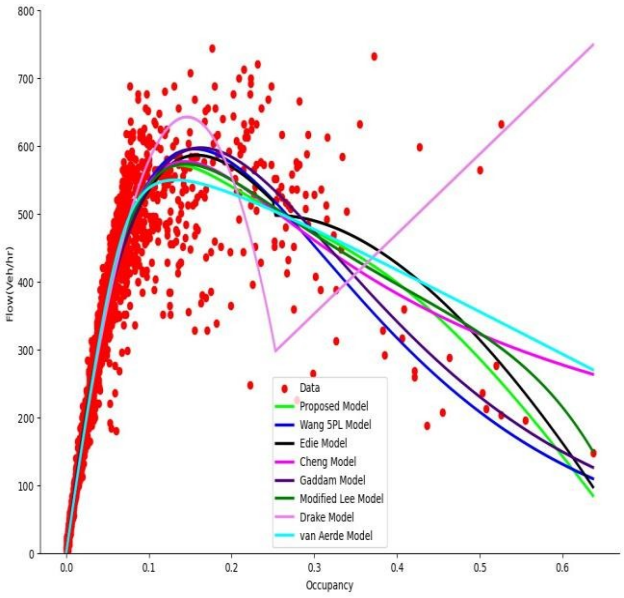

(a) Flow density curves for Canada/Toronto/N30431H2

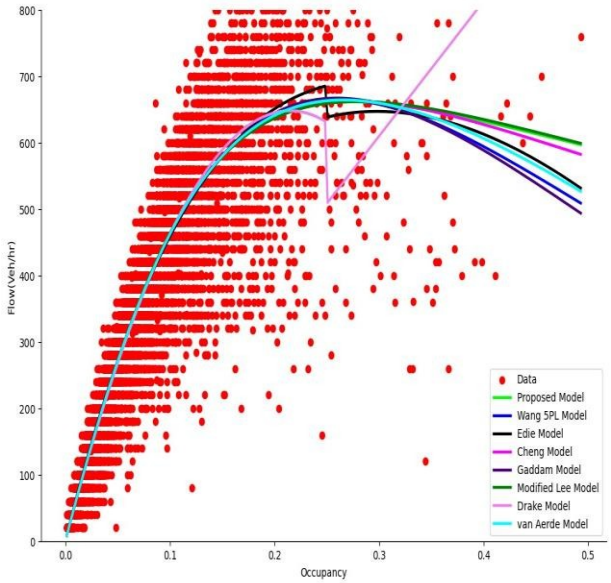

(b) Flow-density curves for France/Merseille/00034PMA0001

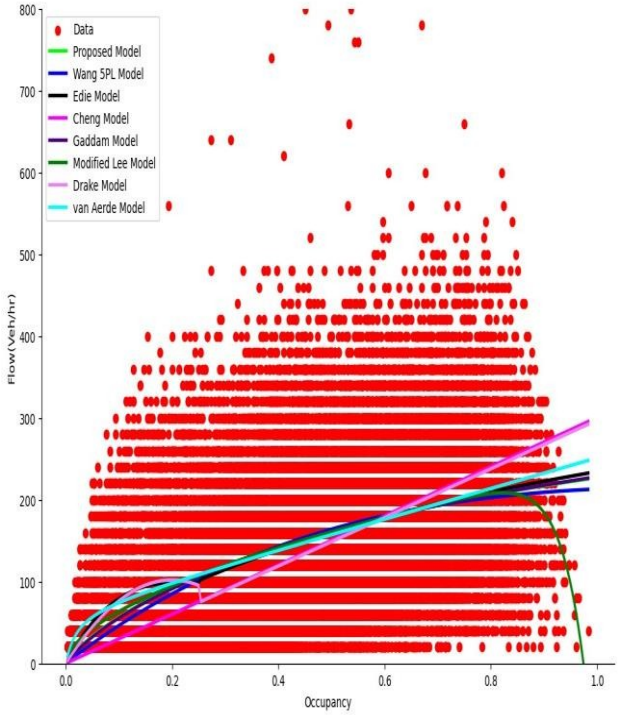

(c) Flow-density curves for Germany/Hamburg/K1225D3_2

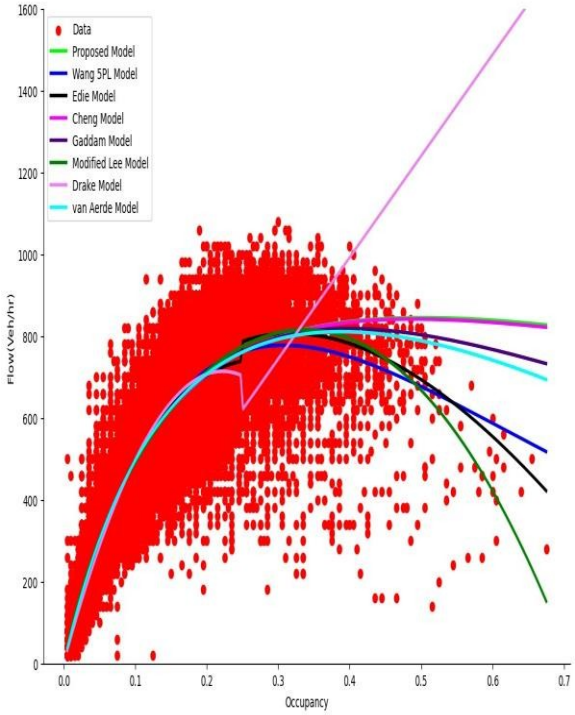

(d) Flow-density curves for Switzerland/Luzern/ ig11FD107_D3

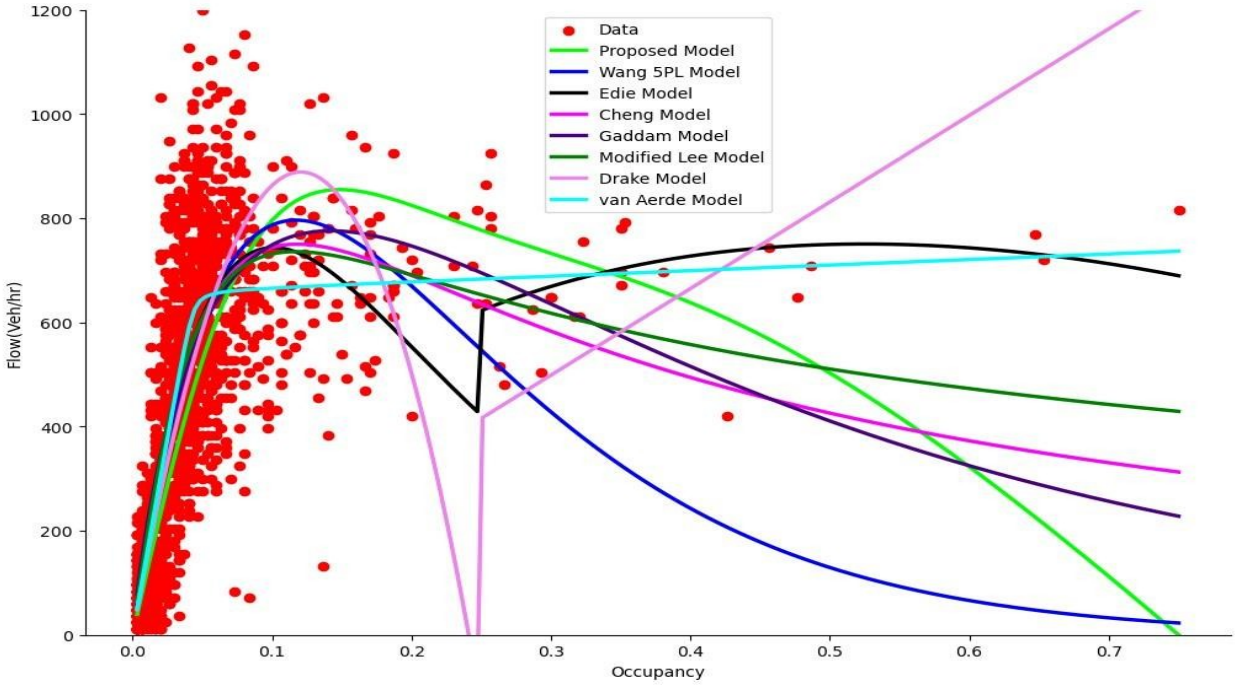

(e) Flow-density curves for France/Bodeaux/ Z28CT7

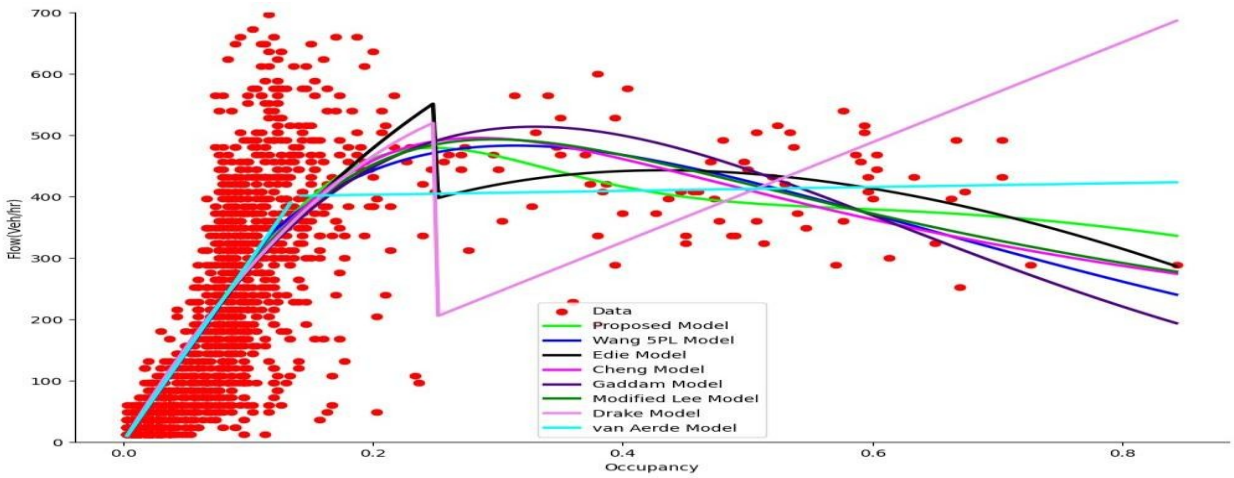

(f) Flow-density curves for France/Bodeaux/ Z224CT13

Fig. 4. Curve fits of the proposed models and some selected models on the data from different roads using Levenberg-Marquardt (LM)

Discussions

The average RMSE in Table 3 shows that the proposed model has better predictive power as it has the lowest value followed by Cheng's model. This means that the model can generalize easily. From the plots, Fig. 2a and b, the performance of the proposed model compares well on both the training and test data. The two graphs are undistinguishable unlike, for example, van Aerde model which has the highest average RMSE showing striking difference in both the training and test data as seen in Fig. 2. The graph on the test data shows the van Aerde's model overestimates the flow significantly. This result proves that the excellent performance of the proposed model is not attributed to over fitting while that of van Aerde model is due to over fitting. Similarly, a closer look at the performances of all the other models on the test data further reveals their poor performance at mid and high densities. This indicates that most of the models cannot be used to predict flows at mid and high densities with good accuracy. Interestingly, this range of density is mostly lacking and/or scarce/sparsely available in most traffic data. The proposed model may, therefore, be a handy tool in this regard, i.e. it will useful for extrapolation of traffic states at mid and high densities.

Fig. 3 shows that all the model perform relatively well in all the six roads examined except Cheng's model, which did poorly on road 3 and this is also clearly seen in Fig. 4c. The reason for this performance by all the models may not be unconnected with the fact that the data in most of the roads barely cover the free-flow regime only. This is not surprising because most models' performance at low densities is good and similar and only begins to show variation at mid and high densities. Therefore, to properly assess the transferability of these models, roads with full range of data i.e. from light traffic to congested traffic are required. A careful examination of Fig. 4a to f reveals the consistency of the proposed model in mimicking the empirical fundamental diagrams despite the variation in data distribution. This proves that the proposed model has high flexibility that enables it to adapt to most trends of traffic data despite its few parameters.

Conclusion

K-fold cross-validation was used to assess and compare the predictive performance of some macroscopic equilibrium fundamental diagram with a newly proposed model. The results reveal that the newly proposed model perform better than the other models in predicting traffic states, particularly, in mid and high densities. This shows that the proposed model could be useful for

extrapolation of traffic states at mid and high densities. Furthermore, the proposed model shows consistently good performance across various roads despite its few parameters. This proves that the proposed model has high flexibility that enables it to adapt to most trends of traffic data.

References

[1] D. M. Bramich, M. Menendez, and L. Ambuhl, "Fitting Empirical Fundamental Diagrams of Road Traffic: A Comprehensive Review and Comparison of Models Using an Extensive Data Set," *IEEE Trans. Intell. Transp. Syst.*, vol. 23, no. 9, pp. 14104–14127, 2022a, doi: 10.1109/TITS.2022.3142255.
[2] Q. Cheng, Z. Liu, Y. Lin, and X. (Simon) Zhou, "An s-shaped three-parameter (S3) traffic stream model with consistent car following relationship," *Transp. Res. Part B Methodol.*, vol. 153, pp. 246–271, Nov. 2021, doi: 10.1016/j.trb.2021.09.004.
[3] G. Dahiya, Y. Asakura, and W. Nakanishi, "Analysis of the single-regime speed-density fundamental relationships for varying spatiotemporal resolution using Zen Traffic Data," *Asian Transp. Stud.*, vol. 8, p. 100066, 2022, doi: 10.1016/j.eastsj.2022.100066.
[4] H. K. Gaddam and K. R. Rao, "Speed–density functional relationship for heterogeneous traffic data: a statistical and theoretical investigation," *J. Mod. Transp.*, vol. 27, no. 1, pp. 61–74, Mar. 2019, doi: 10.1007/s40534-018-0177-7.
[5] M. Y. Mafuyai, D. D. Bakwa, and Y. Y. Jabil, "A Single-Regime Fundamental Diagram of Vehicular Traffic with Excellent Performance at All Traffic States." 2024. doi: 10.2139/ssrn.4777787.
[6] M. J. Cassidy, "Bivariate relations in nearly stationary highway traffic," *Transp. Res. Part B Methodol.*, vol. 32, no. 1, pp. 49–59, 1998, doi: 10.1016/S0191-2615(97)00012-X.
[7] J. M. Del Castillo and F. G. Benitez, "On the functional form of the speed-density relationship—I: General theory," *Transp. Res. Part B Methodol.*, vol. 29B, no. 5, pp. 373–389, Oct. 1995, doi: 10.1016/0191-2615(95)00008-2.
[8] J. S. Drake, J. L. Schofer, and A. D. May, "A Statistieal Analysis of Speed Density Hypotheses," *Veh. Traffic Sci.*, vol. 154, pp. 112–117, 1967.
[9] L. C. Edie, "Car-Following and Steady-State Theory for Noncongested Traffic," *Oper. Res.*, vol. 9, no. 1, pp. 66–76, 1961.
[10] H. M. Zhang, "Amathematical theory of traffic hysteresis," *Transp. Res. Part B*, vol. 33, pp. 1–23, 1999.
[11] H. Wang, J. Li, Q.-Y. Chen, and D. Ni, "Logistic modeling of the equilibrium speed–density relationship," *Transp. Res. Part Policy Pract.*, vol. 45, no. 6, pp. 554–566, Jul. 2011, doi: 10.1016/j.tra.2011.03.010.
[12] D. M. Bramich, M. Menendez, and L. Ambuhl, "Fitfun: A modelling framework for successfully capturing the function form and noise of observed traffic flow-density-speed relationships," *Transp. Res. Part C*, vol. 151, p. 104068, 2023, doi: 10.1016/j.trc.2023.104068.
[13] A. Romanowska and K. Jamroz, "Comparison of Traffic Flow Models with Real Traffic Data Based on a Quantitative Assessment," *Appl. Sci.*, vol. 11, no. 21, p. 9914, Oct. 2021, doi: 10.3390/app11219914.
[14] D. Ni, J. D. Leonard, C. Jia, and J. Wang, "Vehicle Longitudinal Control and Traffic Stream Modeling," *Transp. Sci.*, vol. 50, no. 3, pp. 1016–1031, Aug. 2016, doi: 10.1287/trsc.2015.0614.
[15] R. Kucharski and A. Drabicki, "Estimating Macroscopic Volume Delay Functions with the Traffic Density Derived from Measured Speeds and Flows," *J. Adv. Transp.*, vol. 2017, pp. 1–10, Feb. 2017, doi: 10.1155/2017/4629792.
[16] Y. Wang *et al.*, "Macroscopic traffic flow modelling of large-scale freeway networks with field data verification: State-of-the-art review, benchmarking framework, and case studies using METANET," *Transp. Res. Part C*, vol. 145, Oct. 2022, doi: https://doi.org/10.1016/j.trc.2022.103904.
[17] Greenshields, B.D., "A study of traffic capacity," *Proc Highw. Res Board*, vol. 14, pp. 448–477, 1935.
[18] D. R. Drew, *Traffic flow theory and control*. New York: McGraw-Hill, 1968.
[19] L. A. Pipes, "Car following models and the fundamental diagram of road traffic," *Transp. Res.*, vol. 1, no. 1, pp. 21–29, May 1967, doi: 10.1016/0041-1647(67)90092-5.
[20] A. D. May and M. Keller, "Non-Integer Car-Following Models," *Highw Res Rec*, vol. 199, pp. 19–32, 1967.

[21] R. Jayakrishnan, W. K. Tsai, and A. Chen, "A dynamic traffic assignment model with traffic-flow relationships," *Transp. Res. Part C Emerg. Technol.*, vol. 3, no. 1, pp. 51–72, Feb. 1995, doi: 10.1016/0968-090X(94)00015-W.
[22] H. Greenberg, "An Analysis of Traffic Flow," *Oper. Res.*, vol. 7, no. 1, pp. 79–85, Feb. 1959.
[23] R. T. Underwood, "Speed, volume and density relationships," in *Quality and Theory of Traffic flow*, Yale University, New Haven, Connecticut: Bureau of highway Traffic, 1961, pp. 141–188.
[24] M. Papageorgiou, J.-M. Blosseville, and H. Hadj-Salem, "MACROSCOPIC MODELLING OF TRAFFIC FLOW ON THE BOULEVARD PfiRIPHgRIQUE IN PARIS," *Transp. Res. Part B*, vol. 23B, no. 1, pp. 29–47, 1989.
[25] Franklin, R.E., "The structure of a traffic shock wave," *Civ. Eng Public Works Rev*, vol. 56, no. 1186–1188, 1961.
[26] G. F. Newell, "Nonlinear Effects in the Dynamics of Car Following," *Oper. Res.*, vol. 9, no. 2, pp. 209–229, Apr. 1961, doi: 10.1287/opre.9.2.209.
[27] Kerner, B.S. and Konhauser, P., "Structure and parameters of cluster in traffic flow," *Phys. Rev. E*, vol. 50, no. 1, pp. 54–86, Jul. 1994.
[28] H. Y. Lee, H. W. Lee, and D. Kim, "Origin of synchronized raffic flow on highways and its dynamic phase transitions.," *Phys Rev Lett*, vol. 81, no. 5, pp. 1130–1133, 1998, doi: 10.1103/physRevLstt.81.1130.
[29] A. E. Boardman and L. B. Lave, "Highway congestion and congestion tolls," *J Urban Econ*, vol. 4, pp. 340–359, 1977, doi: 10.1016/0094-1190(77)90016-X.
[30] van Aerde, M., "A single regime speed-flow-density for freeways and arterials," pp. 1–19, 1995.
[31] Bando, M., Hasebe, K., Nakayama, A., Shibata, A., and Sugiyama, Y, "Dynamical model of traffic congestion and numerical simulation," *Phys. Rev. E*, vol. 51, no. 2, Feb. 1995.
[32] Ghandehari, M. and Ardekani, S., "A modified greeberg speed-flow traffic model," *Dept Math Univ Tex. Arlingt. Arlinton TX USA Tech Rep*, vol. 357, 2008.
[33] MacNicholas, M.J., "A simple pragmatic representation of traffic flow," *Tansp. Res. Circular*, pp. 161–177, 2008.
[34] D. C. Gazis, R. Herman, and R. B. Potts, "Car-Following Theory of Steady-State Traffic Flow," *Oper. Res.*, vol. 7, no. 4, pp. 499–505, Aug. 1959.
[35] X. Qu, S. Wang, and J. Zhang, "On the fundamental diagram for freeway traffic: A novel calibration approach for single-regime models," *Transp. Res. Part B Methodol.*, vol. 73, pp. 91–102, Mar. 2015, doi: 10.1016/j.trb.2015.01.001.
[36] F. L. Hall, "Traffic Stream Characteristics," in *Traffic Flow Theory: A State-of-the-art Report*, 2nd ed., Tranportation Research Board's Committee A3A11, 2001, p. 2.1-2.34.
[37] N. Maiti and B. R. Chilukuri, "Empirical Investigation of Fundamental Diagrams in Mixed Traffic," *IEEE Access*, vol. 11, pp. 13293–13308, 2023, doi: 10.1109/ACCESS.2023.3242971.
[38] A. C. Dick, "Speed/flow relatioships within an urban area," *Traffic Eng Control*, vol. 8, pp. 393–396, 1966.
[39] P. K. Munjal, Y. S. Hsu, and R. L. Lawrence, "Analysis and validation of lane-drop effects on multi-lane freeways," *Transp. Res.*, vol. 5, pp. 257–266, 1971, doi: 10.1016/0041-1647(71)90037-2.
[40] S. A. Smulder, *Control of Freeway Traffic Flow*. Amsterdam, The Netherlands: Stichting Mathematisch Centrum, 1989.
[41] A. D. May, *Traffic Flow Fundamentals*. Prentice Hal, 1990.
[42] C. F. Daganzo, "Fundamentals of Transportation and Traffic Operations," Emerald: Bingley, UK., 1997.
[43] N. Wu, "A new approach for modeling of Fundamental Diagrams," 2002.
[44] D. M. Bramich, M. Menendez, and L. Ambühl, "Road traffic time-series measurements of flow and occupancy from 10,150 loop detectors in 25 cities," Harvard Dataverse, 2022b. [Online]. Available: https://dataverse.harvard.edu